Electron-spin-resonance center of dangling bonds in undoped *a*-Si:H

T. Umeda
Joint Research Center for Atom Technology (JRCAT), National Institute for Advanced Interdisciplinary Research (NAIR), 1-1-4, Higashi, Tsukuba, 305, Japan
and Institute of Materials Science, University of Tsukuba, Tsukuba, 305, Japan

S. Yamasaki
Joint Research Center for Atom Technology (JRCAT), National Institute for Advanced Interdisciplinary Research (NAIR), 1-1-4, Higashi, Tsukuba, 305, Japan

J. Isoya
Joint Research Center for Atom Technology (JRCAT), National Institute for Advanced Interdisciplinary Research (NAIR), 1-1-4, Higashi, Tsukuba, 305, Japan
and University of Library and Information Science, 1-2 Kasuga, Tsukuba, 305, Japan

K. Tanaka
Joint Research Center for Atom Technology (JRCAT), National Institute for Advanced Interdisciplinary Research (NAIR), 1-1-4, Higashi, Tsukuba, 305, Japan
and Institute of Materials Science, University of Tsukuba, Tsukuba, 305, Japan

(Received 5 October 1998)

A variety of electron-spin-resonance (ESR) spectra of dangling bond ($g=2.0055$) in undoped hydrogenated amorphous silicon (*a*-Si:H) have been measured by the echo-detected ESR of pulsed ESR as well as the usual continuous-wave (cw) ESR for a wide range of two experimental parameters of microwave frequency ($\nu=3-34$ GHz) and ^{29}Si content ($p=1.6$, 4.7, 9.1 at. %). Using those spectra, we have carried out spectral simulations on the whole dangling bond spectrum (a primary line and ^{29}Si hf structure), and also have simulated ν and p dependence of the spectra. From detailed simulation analyses, we confirmed a previous identification of the dangling bond center by Stutzmann and Biegelsen [Phys. Rev. B **40**, 9834 (1989)], and raised the reliability of ESR parameters; isotropic and anisotropic ^{29}Si hyperfine interactions were determined to be approximately 7.4 and 2.1 mT, respectively, and $g_{\parallel}=2.0039$, $g_{\perp}=2.0065$. The ESR parameters indicate that the dangling bond center is localized predominantly on a single Si atom and is characterized as strongly p like, which are consistent with the case of the dangling bond at the interface between crystalline Si and SiO_2, the P_b center. [S0163-1829(99)01307-7]

I. INTRODUCTION

Amorphous silicon (*a*-Si) and hydrogenated amorphous silicon (*a*-Si:H) contain threefold-coordinated Si atoms, i.e., dangling bonds (DB's) with a density of 10^{18-20} and $10^{15-18}\,\mathrm{cm}^{-3}$ for *a*-Si and *a*-Si:H, respectively.[1,2] The incorporation of a great number of hydrogen (10–20 at. %) greatly reduces the DB's.[2] However, low-defect-density ($<10^{17}\,\mathrm{cm}^{-3}$) *a*-Si:H responds with the creation of additional metastable DB's to strong illumination.[3–5] The metastable DB's are created in bulk regions up to a density of $10^{17}\,\mathrm{cm}^{-3}$ and can be annihilated completely by thermal annealing ($\geqslant 150\,^{\circ}\mathrm{C}$). The microscopic mechanism of such creation and annihilation has not been clarified yet, although they were discovered more than 20 years ago. Therefore, microscopic and electronic structures of the DB's have been investigated intensively, and further information is still required.

The DB in *a*-Si:H shows an electron-spin-resonance (ESR) signal with a g value (g) of 2.0055,[1,4] which is shown in Fig. 1. This signal involves weak signals of the hyperfine (hf) structure of ^{29}Si (natural abundance of 4.7 at. %, nuclear spin of $I=\frac{1}{2}$) which are indicated by arrows in the figure, in addition to a strong primary line. ^{29}Si hf splittings originate from the magnetic interactions between ^{29}Si nuclei and an unpaired electron, from which the distribution of the unpaired electron relative to positions of ^{29}Si nuclei can be revealed. For example, for DB's on the surface of crystalline Si(111) covered by SiO_2, the P_b centers also show a ^{29}Si hf structure in their ESR spectrum. Detailed analyses clarified that an unpaired electron of the P_b center distributes on one Si atom by 82% where the electron wave function consists of $3s$ and $3p$ orbitals of approximately 10% and 90%, respectively.[6,7] On the other hand, the DB spectrum of *a*-Si:H convolutes the powder pattern as well as causes a large signal broadening due to its amorphous nature. Therefore, it is difficult to determine principal values of the hf and g tensors, unlike the case of the P_b center.

A first analysis on ^{29}Si hf interactions of the DB center in *a*-Si:H was reported by Biegelsen and Stutzmann.[8] They observed doublet ^{29}Si hf lines using a heavily ^{29}Si-enriched (93 at. %) sample and determined the isotropic part (A_{iso}) of the strong ^{29}Si hf interaction from which the fraction of the $3s$ orbital in the DB wave function was estimated for the first

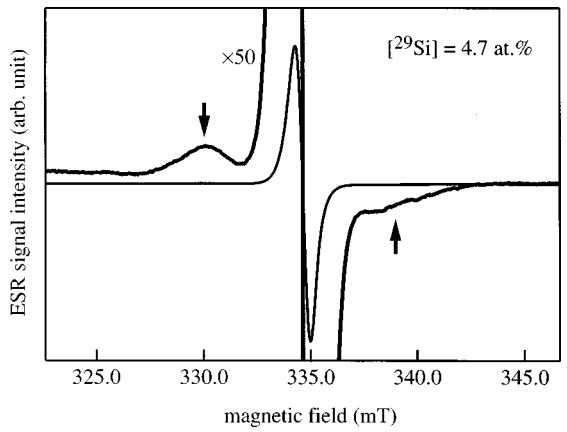

FIG. 1. A typical DB spectrum of undoped a-Si:H with [^{29}Si] = 4.7 at.% and a spin density of 3.6×10^{18} cm^{-3}. The spectrum was measured by a standard X-band (9.4-GHz) continuous wave (cw)-ESR spectrometer with 2.5 h accumulation. Arrows point to hf lines of ^{29}Si.

time.[9] In their sample, however, there existed a large number of ^{29}Si nuclei surrounding a DB site, which caused an extreme broadening of the signal due to weak ^{29}Si hf splittings. Such a signal broadening smeared out finer features of the strong ^{29}Si hf interaction. Following the first work, Stutzmann and Biegelsen carried out a detailed simulation of an X-band (~10 GHz) ESR spectrum of a natural abundance sample,[9] from which further detailed information was extracted such as the anisotropic hf interaction ($A_{\rm aniso}$) due to the $3p$ orbital in the DB wave function. As a result, they reported that the DB center in a-Si:H has approximately 50% of the distribution on one Si atom, which consists of $3s$ and $3p$ orbitals of approximately 10 and 90 %, respectively. They concluded that the origin of $g=2.0055$ center is well described as the DB, although five-fold-coordinated Si atoms, so-called ''floating bonds'' (FB's),[10] had been suggested for an alternative origin of $g=2.0055$ and the two models had been argued intensely.[10–18]

However, since tails of the strong primary line are superposed on hf lines in Fig. 1, it was very difficult to accurately deconvolute the ^{29}Si hf structure from the total spectrum. In order to remove tails of the strong primary line, they made a great effort to choose a smooth, structureless tail curve that joins the main peak of the primary line continuously. The tail curve was chosen by satisfying three qualifications; (i) it had no structure in the second derivative over the region of ^{29}Si hf lines, and when the tail curve had been subtracted from the total spectrum, (ii) deconvoluted hf lines returned to zero for separating each hf line, and (iii) each hf line had an equal area.[9] Choosing a suitable tail curve, they seemed to obtain the deconvoluted hf structure successfully. We point out, however, that the best approach is to calculate the whole DB spectrum (the primary line and ^{29}Si hf lines) without deconvoluting hf lines, because the results may depend on how the tail curve is chosen. Furthermore, in order to confirm the reliability of ESR parameters determined in the simulation, it will be necessary to check the simulations for a variety of the DB spectra; Stutzmann and Biegelsen carried out the spectral simulation for only one X-band spectrum.

In this paper, we present a detailed simulation study to confirm the conclusion of Stutzmann and Biegelsen.[9] Our simulations have two features: (a) simulations of the whole DB spectrum (a primary line and ^{29}Si hf lines), and (b) simulations of the dependence of the DB spectrum on two experimental parameters of microwave frequency (3–34 GHz) and ^{29}Si content of the sample (1.6, 4.7, 9.1 at %). The two experimental parameters can increase (or reduce) influences of particular ESR parameters on the DB spectrum. Furthermore, we employed the echo-detected ESR technique of pulsed ESR in order to obtain the ESR spectrum with much flatter baselines than that of conventional, continuous-wave (cw)-ESR, which is advantageous for analyzing the weak signal of ^{29}Si hf lines. From detailed simulation analyses over a wide range of the two experimental parameters, principal values of the g and hf tensors, $A_{\rm iso}$ and $A_{\rm aniso}$ were determined with high reliability. Finally, we compare our results with those of Stutzmann and Biegelsen as well as those for the P_b center.

TABLE I. List of our samples and their characters.

Sample	^{29}Si (at. %)	^{1}H (at. %)	N_s (cm^{-3})
T_s = R.T.	1.6	30.3	9.4×10^{17}
	4.7	11.8	3.6×10^{18}
	9.1	23.7	1.3×10^{18}
T_s = 250 °C	1.6	8.9	6×10^{15}
	4.7	6.8	1×10^{15}
	9.1	10.7	4×10^{15}

II. EXPERIMENTAL DETAILS

Most of the ESR measurements on a-Si:H have been carried out by a standard X-band (9–10 GHz) spectrometer so far.[1,2,8,9,12,14,19] In the present work, we used microwave frequencies of 3.0–34 GHz. The microwave frequency of ν is simply related with the resonance magnetic field of B_r by $h\nu=g\beta B_r$, where h is the Planck constant and β is the Bohr magneton. Therefore, the primary line, which is broadened mainly by the anisotropy of principal g values (i.e., powder pattern) and fluctuations of g values, can be narrowed by decreasing ν, while the hf splitting does not change.[4] Thus, the degree of overlapping of the primary line and hf lines can be experimentally controlled by changing ν.

Another parameter, the ^{29}Si contents of the sample (p), can determine the relative intensity of hf lines in a total spectrum. We varied the value of p to 1.6 (diluted), 4.7 (natural abundance), and 9.1 (enriched) at. %.

Undoped a-Si:H samples were deposited by the standard rf-glow discharge technique from SiH_4 on a metal foil at substrate temperatures (T_s) of room temperature (R.T.) and 250 °C. Deposited samples (10–40 mg) were collected in high-purity vitreous-silica tubes for ESR measurements. The DB densities (N_s) and hydrogen contents of the samples were determined using ESR and ^{1}H-NMR, which are summarized in Table I.

ESR measurements of the above samples were carried out by cw- and pulsed-ESR spectrometers. In cw-ESR measurements, we used a BRUKER ESP300E spectrometer, which can operate with microwave frequencies of 3.0, 6.5, 9.4–9.8, and 34 GHz. All cw-ESR spectra were measured at room temperature under the following conditions: microwave

powers of 0.1 (34 GHz) and 0.9 mW (3.0, 6.5, 9.8 GHz), field modulation amplitudes in a range from 0.1 mT (3.0 GHz) to 0.7 mT (34 GHz) and 100 kHz of a modulation frequency. In order to get a sufficient signal-to-noise ratio, some spectra were accumulated for several hours.

In pulsed-ESR measurements, we used a home-built pulsed ESR spectrometer that can operate with frequencies of 8.2, 9.4, 11 GHz. The pulse widths were 17 and 34 nsec for 90° and 180° microwave pulses, respectively, and the microwave field B_1 was estimated to be less than 0.52 mT. The echo intensity was accumulated by a 50-nsec-wide boxcar gate and then was digitized by a 12-bit A/D converter. Details of other setups of our spectrometer have been described elsewhere.[20,21] The echo-detected ESR spectra are obtained by recording the amplitude of two-pulse Hahn echo (90° pulse–τ–180° pulse–τ–echo) as a function of magnetic-field strength. The magnetic field increment was either 0.04 or 0.1 mT. The echo-detected ESR spectrum is equivalent to an integrated spectrum of cw ESR except for its much flatter baseline than that of cw ESR because the microwave pulses are not applied at a time of detecting the echo signal and because phase cycling techniques are employed.[20,21] Pulsed-ESR measurements were carried out at 50 K with $\tau = 240$ nsec and 1 msec repetition time of pulse sequences in order to achieve the highest signal-to-noise ratio. The spin echo signal was often smaller than the cw-ESR signal, so that the longest accumulation time was prolonged up to three days.

III. RESULTS AND DISCUSSION

A. Simulation method

It is necessary for determining ESR parameters of the 2.0055 center to perform spectral simulation. We considered the same spin system as the P_b center for the present simulation, namely, (a) the system has an axial symmetry the axis of symmetry of which coincides with the direction of the $3p$ orbital in the DB wave function, (b) the electron spin S is $\frac{1}{2}$ and DB's are isolated from each other,[5,22] and (c) the nuclear spin I is either zero for DB's on ^{28}Si and ^{30}Si atoms, or $\frac{1}{2}$ for DB's on ^{29}Si atoms.[6,7] Although the DB defects in the amorphous network are likely to have g and ^{29}Si hf tensors which slightly deviate from axial symmetry, such minor corrections to our simple model seem to be smeared out by the large signal broadening due to site-to-site variation of structure. Hence we apply the above simple model of axial symmetry.

Under conditions of (a)–(c), an effective g value $g(\theta)$ and a hf splitting $K(\theta)$ are given by[23]

$$g(\theta)^2 = g_{\parallel}^2 \cos^2\theta + g_{\perp}^2 \sin^2\theta \tag{1}$$

and

$$K(\theta)^2 g(\theta)^2 = A_{\parallel}^2 g_{\parallel}^2 \cos^2\theta + A_{\perp}^2 g_{\perp}^2 \sin^2\theta, \tag{2}$$

respectively, where $g_{\parallel}, g_{\perp}$ and $A_{\parallel}, A_{\perp}$ are principal values of the g and hf tensors parallel ($\parallel$) and perpendicular ($\perp$) to the direction of the axis of symmetry, respectively. θ is the angle between the axis of symmetry and the applied magnetic field. Line positions are given by

$$B_r(\theta) = h\nu/g(\theta)\beta \quad \text{for the primary line,} \tag{3a}$$

and

$$B_r^{\pm}(\theta) = h\nu/g(\theta)\beta \pm K(\theta)/2 \quad \text{for the } ^{29}\text{Si hf lines.} \tag{3b}$$

Although we calculated line positions of the hf lines in terms of the second order in K,[23] they were hardly different from the first-order result. Signal intensities $P(\theta)$ are calculated as[24]

$$P(\theta) = g_{\perp}^2 [g_{\parallel}^2/g(\theta)^2 \cos^2\theta + 1]. \tag{4}$$

Finally, the ESR spectrum of $Y(B)$ is given by

$$Y(B) = C \int_0^{\pi/2} d\theta \sin\theta P(\theta) \Big[(1-p) f(B - B_r(\theta), W(\theta)) + \frac{p}{2} f_{\mathrm{hf}}(B - B_r^{+}(\theta), W_{\mathrm{hf}}(\theta)) + \frac{p}{2} f_{\mathrm{hf}}(B - B_r^{-}(\theta), W_{\mathrm{hf}}(\theta)) \Big], \tag{5}$$

where B is the strength of the applied magnetic field, C is a normalizing constant, f and f_{hf} are broadening functions for the primary and hf lines, and $W(\theta)$ and $W_{\mathrm{hf}}(\theta)$ are full width at half-maximum of those functions, respectively.

Stutzmann and Biegelsen calculated separately the first term (the primary line) and the last two (hf lines) in Eq. (5).[9] They deconvoluted the hf lines from a total spectrum using a smooth, structureless tail curve which joins the main peak of the primary line continuously. On the other hand, in the present work, we calculate the whole spectrum from a combination of three terms in Eq. (5) without deconvoluting the hf lines, and analyze the dependence of the spectrum on two experimental parameters of ν and p. As a result, our spectral simulation is not affected by the method of choosing the tail curve and thus the reliability of ESR parameters is increased. Although Stutzmann and Biegelsen adopted the Gaussian broadening function for f and f_{hf} because of random fluctuations arising from the amorphous nature, we need to consider the broadening function in more detail.

It is considered that the signal broadening is caused by two dominant mechanisms: (i) distributions of ESR parameters such as $g_{\parallel}, g_{\perp}, A_{\parallel}, A_{\perp}$ due to site-to-site variation of structures, and (ii) additional hf interactions such as weak ^{29}Si hf interaction from backbonded Si atoms and from more distant Si atoms and weak ^{1}H hf interactions from nearby H atoms.

In regard to the contribution (i), the broadening function may be well described by the Gaussian function because of random fluctuations of parameters. Now, we define $W_{\parallel}^{g}, W_{\perp}^{g}$ and $W_{\parallel}^{A}, W_{\perp}^{A}$ as full widths at half-maximum of Gaussian distributions of $g_{\parallel}, g_{\perp}$ and $A_{\parallel}, A_{\perp}$ in a field dimension, respectively. Equations (3a) and (3b) mean that fluctuations of g and K increase the fluctuation of resonance fields linearly, assuming a small g-shift. Therefore, we assumed simply that full widths at half-maximum of the Gaussian broadening function increase linearly with g and K themselves,[9] then

$$W(\theta)^2 = (W_{\parallel}^{g})^2 \cos^2\theta + (W_{\perp}^{g})^2 \sin^2\theta, \tag{6a}$$

$$W_{\mathrm{hf}}(\theta)^2 = W(\theta)^2 + W_K(\theta)^2, \tag{6b}$$

where

$$W_K(\theta)^2 = (W_{\parallel}^{A})^2 \cos^2\theta + (W_{\perp}^{A})^2 \sin^2\theta. \tag{6c}$$

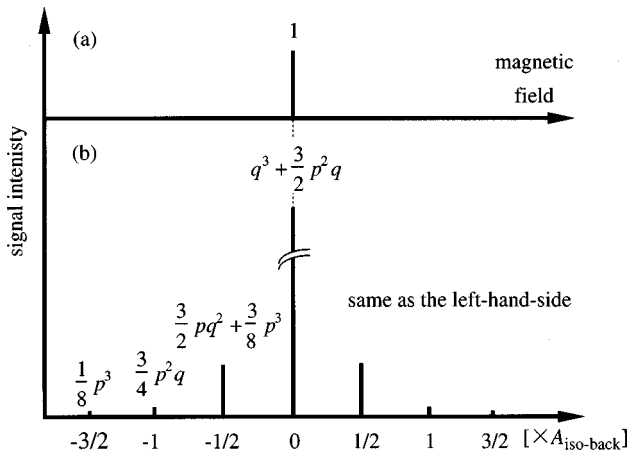

FIG. 2. Illustration of the isotropic hf splittings, $A_{\text{iso-back}}$, due to three backbonded Si atoms. Two figures show the cases (a) before and (b) after taking into account $A_{\text{iso-back}}$ where $q=1-p$.

The validity of Eq. (6a) has been confirmed in the P_b spectrum.[25] Two kinds of broadening parameters of $W_{\parallel}^{g}, W_{\perp}^{g}$ and $W_{\parallel}^{A}, W_{\perp}^{A}$ are different in their dependence on ν. With increasing ν, the former two should increase linearly, while the latter two should remain constant.

The contribution (ii) to W and W_{hf} is classified into two groups. When additional weak hf splittings are comparable with or are greater than the sizes of W and W_{hf}, it may be inappropriate to describe f and f_{hf} by a single Gaussian function. Such additional hf splittings will be caused by the isotropic hf interactions due to ^{29}Si atoms at three backbond sites of a DB.[8,11] Although a first-principles theoretical calculation reported that the next largest isotropic hf splittings are yielded at some of the next-nearest-neighbor sites of the DB, the number of such sites was also counted to be 3.[18] When $A_{\text{iso-back}}$ is defined as the average isotropic hf splitting due to backbonded ^{29}Si, a single line splits into seven lines, as is illustrated in Fig. 2. Furthermore, even if additional hf splittings are rather smaller in size than W and W_{hf}, they will not only increase the broadening width but also affect the line shape. It is known that the line shape is well described by the cutoff Lorentzian curve rather than the Gaussian curve when the density of nuclear spins surrounding the spin center is very small.[26] In fact, it was reported that the line shape of the 2.0055 spectrum as well as the P_b spectrum is well given by the Voigt function, which has a medium curve between the Gaussian and the Lorentzian curves.[14,25] As a result, the broadening widths of $W_{\parallel}^{g}, W_{\perp}^{g}$ have a constant component at $\nu=0$ in addition to the component in proportion to ν, and we evaluated Eq. (5) using a group of seven Voigt functions, $f(B-B_r(\theta),W(\theta),y,A_{\text{iso-back}})$, for the broadening function of the primary line, where y is a shape parameter and details are described in Ref. 27 ($f\rightarrow$Gaussian when $y\rightarrow 0$, $f\rightarrow$Lorentzian when $y\rightarrow\infty$). For the broadening function of hf lines, a group of seven Gaussian functions, $f_{\text{hf}}(B-B_r^{\pm}(\theta),W_{\text{hf}}(\theta),A_{\text{iso-back}})$, was adopted, because hf lines should be greatly influenced by the Gaussian distribution due to large $A_{\parallel}$ and $A_{\perp}$ fluctuations.

The numerical evaluations of Eq. (5) were carried out by a numerical integral with an increment angle $d\theta$ of 0.45°. The calculated spectra were fitted into experimental spectra by non-linear least-squares fitting based on the Levenberg-Marquardt algorithm[28] and, as a result, we determined ESR parameters.

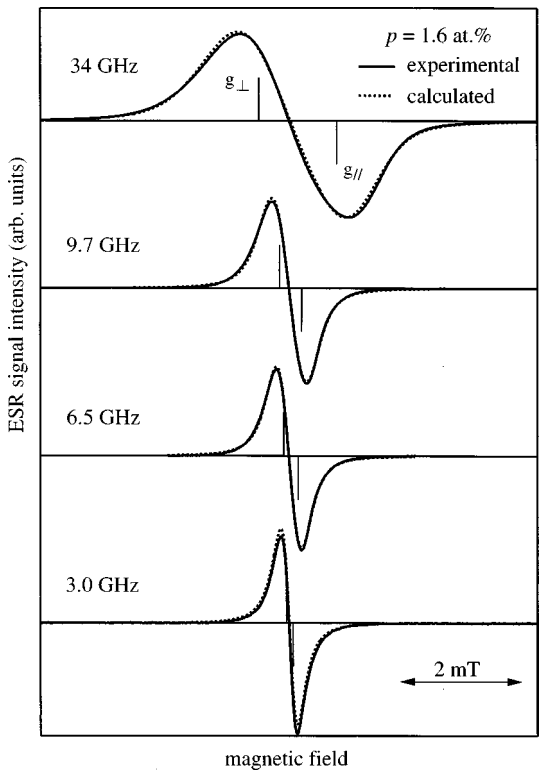

FIG. 3. Cw-ESR spectra of ^{29}Si-diluted undoped a-Si:H ($N_s=9.4\times10^{17}$ cm^{-3}) at various frequencies. Solid and dashed lines indicate experimental and calculated spectra, respectively. The best-fit g parameters are also indicated in the figure.

B. Principal g values and frequency-dependence of the DB spectrum

As the first step, we determined principal g values, because they determine the general shape of the spectrum. The primary line exhibits a slight asymmetry in its line shape that is ascribed to anisotropy of the g tensor.[9] In addition, such anisotropy causes asymmetry of the ^{29}Si hf structure between the low-and high-magnetic-field sides (see Fig. 1).[9]

The overlapping of resonance lines with different g values can be reduced as ν increases.[4] Thus, our Q-band (34-GHz) measurements are more powerful for determining g values than usual X-band (10-GHz) measurements; for example, a 0.001 difference in the g value makes a 0.6-mT difference in resonance fields at 34 GHz as against a 0.17-mT difference for X-band measurements.

Figure 3 shows experimental first-derivative spectra of ^{29}Si-diluted ($p=1.6$ at.%) undoped a-Si:H with $N_s=9.4\times10^{17}$ cm^{-3}, which were obtained by cw-ESR measurements at frequencies of 3.0, 6.5, 9.7, and 34 GHz. This sample is convenient for determining the g parameters because of a lack of the ^{29}Si hf structure.

First, we analyzed the frequency dependence of the line shape and width of the primary line. Peak-to-peak widths of the observed first-derivative spectra $\Delta B_{\text{pp}}(\nu)$ linearly increased with an increase of ν, as is shown in Fig. 4(a). A proportionally increasing component in ΔB_{pp} originates from

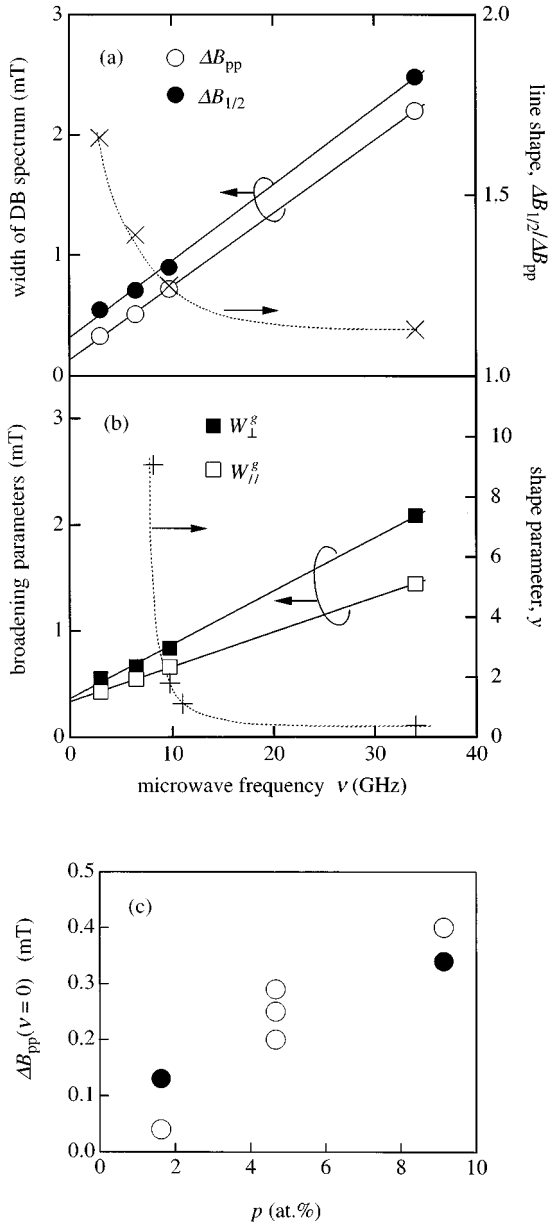

FIG. 4. (a) Frequency dependence of the width and shape of the DB spectra in Fig. 3. Solid lines represent a linearity of ΔB_{pp} (open circles) and $\Delta B_{1/2}$ (closed circles) against ν. A dashed line is a guide to the eyes for $\Delta B_{1/2}/\Delta B_{pp}$ (crosses). (b) Frequency dependence of fitting parameters $W_\parallel^g$ (open squares), $W_\perp^g$ (solid squares), and y (plus symbols). (c) $\Delta B_{pp}(\nu=0)$ plotted against the ^{29}Si contents, p. Solid and open circles correspond to samples with high- (20–30 at. %) and low- (around 10 at. %) hydrogen densities, respectively.

the fluctuations of g values and anisotropy of the g tensor, while a residual component, namely, $\Delta B_{pp}(\nu=0)$, originates mainly from weak hf interactions. We estimated $\Delta B_{pp}(\nu=0)$ of all our samples from the frequency dependence of ΔB_{pp} and plotted them against ^{29}Si contents of the samples p, as shown in Fig. 4(c). The figure clearly shows an appreciable contribution of weak ^{29}Si hf interactions to $\Delta B_{pp}(\nu=0)$. A contribution of ^{1}H hf interactions to the signal broadening was not found, because hydrogen atoms are more than 0.4 nm from the DB site, which corresponds to 0.05 mT of dipolar magnetic fields of ^{1}H.[8,20,29,30]

Figure 4(a) also shows full widths at half maximum of integrated (i.e., absorption) spectra, $\Delta B_{1/2}$. $\Delta B_{1/2}$ increased with the same slope as ΔB_{pp}, while the ratio of ΔB_{pp} to $\Delta B_{1/2}$ decreased as ν increased. This means that as ν increases, the shape of the primary line changes from the Lorentzian curve ($\Delta B_{1/2}/\Delta B_{pp}=1.73$) to the Gaussian curve ($\Delta B_{1/2}/\Delta B_{pp}=1.18$). In other words, at low ν, the line shape is determined to be the Lorentzian curve due to the influence of weak hf splittings. On the contrary, the Gaussian fluctuations of g values dominate at high ν.

In order to determine principal g values from the observed spectra in Fig. 3, we carried out the simulation of the spectra as follows. In this sample, we could simulate the ESR spectrum without including the discernible ^{29}Si hf structure and by neglecting the line splittings due to ^{29}Si hf interactions of backbonded Si atoms. Namely, the first term in Eq. (5) was only calculated and we need not consider a number of small hf lines as shown in Fig. 2(b). Fitting parameters were $g_\parallel, g_\perp, W_\parallel^g, W_\perp^g, C, y$, where both $g_\parallel$ and $g_\perp$ were set to be common for all the spectra. In Fig. 3, the simulated spectra are shown by dashed lines. The simulation minimized the sum of deviations among four experimental and fitted spectra, the so-called χ-square method. Figure 4(b) shows the linearity of $W_\parallel^g$ and $W_\perp^g$ with respect to ν, in which residual components at $\nu=0$ are thought to arise from unresolved weak hf splittings. The angular dependence of the unresolved weak hf splittings seems to be very small because of $W_\parallel^g \sim W_\perp^g$ at $\nu=0$. Finally, principal values of the g tensor were determined to be

$$g_\parallel = 2.0037 - 2.0042 (2.0039), \tag{7a}$$

$$g_\perp = 2.0060 - 2.0067 (2.0065), \tag{7b}$$

respectively, where values in brackets produced the best fitting. The deviations from the best values correspond to about a 50% increase in the χ-square value from its minimum value.

Further discussion will appear in the last section in connection with the discussion on other ESR parameters.

C. ^{29}Si hyperfine interactions

In order to determine principal values of the hf tensor $A_\parallel$ and $A_\perp$, we simulated the whole DB spectra of ^{29}Si enriched ($p=9.1$ at. %) sample by fully calculating Eq. (5). The DB spectra were obtained by the echo-detected ESR technique of pulsed ESR instead of cw ESR. Since the ^{29}Si hf structures for high- and low-spin-density samples are believed to be almost the same,[5,8,9,12] we analyzed the ^{29}Si hf structure of the sample with $N_s = 1.3\times10^{18}\,\mathrm{cm}^{-3}$.

In Fig. 5, solid lines indicate the echo-detected ESR spectra at frequencies of 8.2 and 11 GHz in the first-derivative form. Those spectra were differentiated in order to clarify the detailed features of the ^{29}Si hf structure. As is shown in the figure, two spectra were different in the degree of overlapping of the primary and hf lines. Our simulation calculated two spectra simultaneously in order to reduce arbitrariness in the determination of hf parameters. In the procedure of the simulation, $g_\parallel$ and $g_\perp$ were fixed to values given by Eqs. (7a) and (7b), and fitting parameters were $W_\parallel^g$, $W_\perp^g$, y, $A_{\text{iso-back}}$,

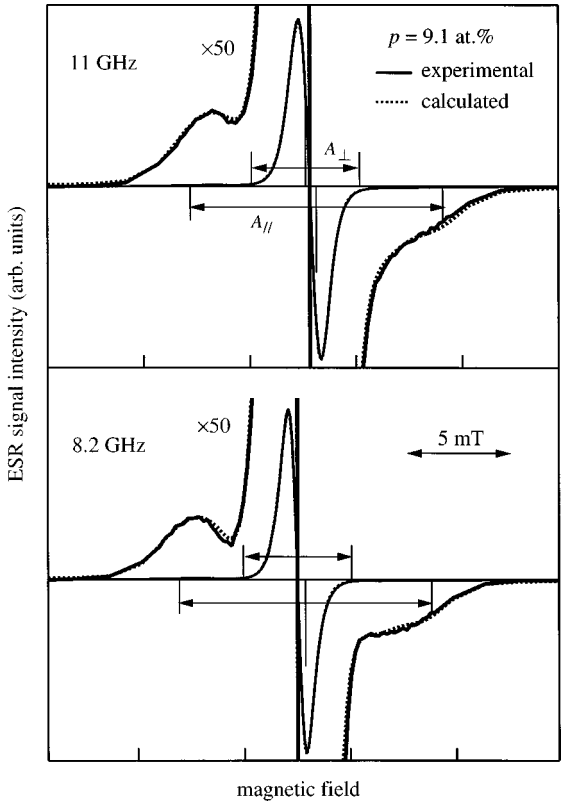

FIG. 5. Echo-detected ESR spectra of ^{29}Si-enriched undoped a-Si:H with $N_s = 1.3\times10^{18}\,\mathrm{cm}^{-3}$ at frequencies of 8.2 and 11, GHz (solid lines) and corresponding simulated spectra (dashed lines). The best-fit hf parameters are also indicated in the figure.

$A_\parallel$, $A_\perp$, $W_\parallel^A$, $W_\perp^A$, and C. Among those parameters, frequency-independent parameters, $A_\parallel$, $A_\perp$, $W_\parallel^A$, $W_\perp^A$, and $A_{\text{iso-back}}$ were set to be common for two spectra. As is shown in Fig. 5, an excellent fitting was obtained, from which principal values of the hf tensor were determined to be

$$A_\parallel = 10.8\text{–}12.3\ \ (11.9)\ \ \mathrm{mT}, \tag{8a}$$

$$A_\perp = 4.9\text{–}5.6\ \ (5.1)\ \ \mathrm{mT}, \tag{8b}$$

respectively, where the best-fit values are in the brackets and deviations of parameters were obtained by the same procedure as the case of g principal values. $A_{\text{iso-back}}$ was estimated to be 1–2 mT. The broadening widths $W_\parallel^A$ and $W_\perp^A$ were approximately 2.6 and 2.0 mT, respectively. In addition, we have examined the parameters given in Eqs. (8a) and (8b) employing samples with ($p = 4.7$ at. %, $N_s = 3.6\times10^{18}\,\mathrm{cm}^{-3}$) and ($p = 1.6$ at. %, $N_s = 9.6\times10^{17}\,\mathrm{cm}^{-3}$), which is shown in Fig. 6. Even for the case of $p = 0.016$, the echo-detected spectra involve the ^{29}Si hf structure clearly at the tail region, although it was not detected by cw ESR. Dashed lines in the figure indicate the simulated spectra that were calculated using the values of $g_\parallel, g_\perp, A_\parallel, A_\perp, A_{\text{iso-back}}$ determined above. As is seen in the figure, the simulations are successful enough to ensure a high reliability of the hf parameters obtained here.

The linear combination of atomic orbitals (LCAO) picture is quite useful for describing the wave function of localized centers in covalently bonded semiconductors.[6–9] When the

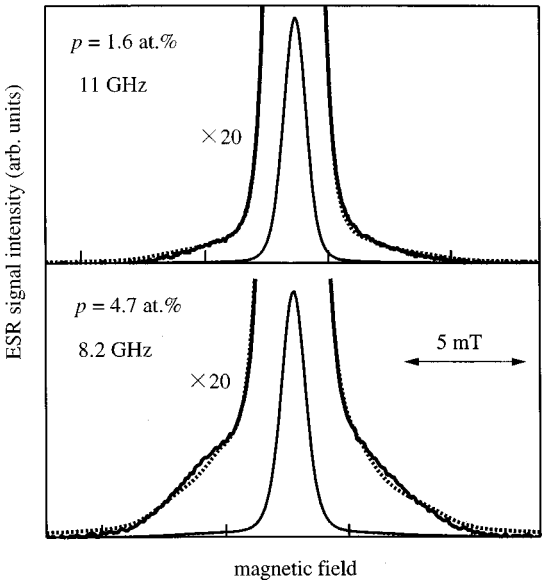

FIG. 6. Echo-detected ESR spectra of ^{29}Si-diluted sample ($p = 1.6$ at. %, $N_s = 9.4\times10^{17}\,\mathrm{cm}^{-3}$) and natural abundance sample ($p = 4.7$ at. %, $N_s = 3.6\times10^{18}\,\mathrm{cm}^{-3}$) with a magnetic-field increment of 0.1 mT (solid lines). Simulated spectra are also shown by dashed lines.

DB wave function is composed of $3s$ and $3p$ orbitals of the Si atom, the hf splitting $K(\theta)$ is written as $K(\theta) = A_{\text{iso}} + A_{\text{aniso}}(3\cos^2\theta - 1)$,[9] where A_{iso} and A_{aniso} are the isotropic and anisotropic ^{29}Si hf splittings due to $3s$ and $3p$ orbitals of the DB, respectively. Thus, A_{iso} and A_{aniso} are given in terms of $A_\parallel$ and $A_\perp$ as

$$A_{\text{iso}} = (A_\parallel + 2A_\perp)/3 = 6.9\text{–}7.9\ \ \mathrm{mT} \tag{9a}$$

and

$$A_{\text{aniso}} = (A_\parallel - A_\perp)/3 = 1.8\text{–}2.5\ \ \mathrm{mT}. \tag{9b}$$

Full widths at half maximum of the distributions of A_{iso} and A_{aniso} were estimated to be $W_{\text{iso}}^A = \frac{1}{3}[(W_\parallel^A)^2 + 4(W_\perp^A)^2]^{1/2} = 1.6\,\mathrm{mT}$ and $W_{\text{aniso}}^A = \frac{1}{3}[(W_\parallel^A)^2 + (W_\perp^A)^2]^{1/2} = 1.1\,\mathrm{mT}$, respectively.

D. ESR parameters—present versus previous work

Up to now, we have determined various ESR parameters. In this section, we compare the present results with previous works of Stutzmann and Biegelsen as well as theories.

Table II summarizes ESR parameters of the 2.0055 center as well as the P_b center obtained by ESR (and related methods) and theoretical calculations. On the whole, each ESR parameter obtained here is similar to that of Stutzmann and Biegelsen.[8,9] Note that A_{iso} and A_{aniso}, which are the most important ESR parameters for determining electronic and microscopic structures of the center, were quite consistent with their previous conclusions. Therefore, with high reliability over a wide range of microwave frequency and ^{29}Si content, our experiments support a previous conclusion of Stutzmann and Biegelsen, namely, that the origin of the 2.0055 center is well identified as the DB. Due to the nature of the DB, the DB center should have a unique Si atom where an unpaired electron is mainly localized and causes

TABLE II. ESR parameters of the 2.0055 center and the P_b center reported by ESR and theoretical works. N and N_{back} represent a number of Si atoms accompanied with the largest and the next largest isotropic ^{29}Si hf interaction, respectively. For atoms counted into N_{back}, their positions are referred to either NN (the nearest-neighbor sites, i.e., backbond sites) or NNN (the next-nearest-neighbor sites). The other parameters are defined in the text. Values in brackets were given by assumptions.

Ref.	$g_{\parallel}$	$g_{\perp}$	N	A_{iso} (mT)	A_{aniso} (mT)	N_{back} & position	$A_{\text{iso-pact}}$ (mT)
			The 2.0055 center in undoped a-Si:H				
(ESR, etc.)							
Present	2.0037–2.0042	2.0060–2.0067	(1)	6.9–7.9	1.8–2.5	(3)	1–2
Refs. 8, 9	2.0038–2.0042	2.0076–2.0084	(1)	7.0–7.5	1.5–2.0	(3)	2–3
Ref. 11[a]				6.9–7.3			2.4–2.8
(Theory)							
Ref. 18[b]			1	10.1	1.8–2.9	3 NNN	1.5
Ref. 18[c]			2	6.0–8.9	0.3–0.5	2 NN	3.2–4.8
Ref. 33[d]	2.0023	2.0037–2.0049					
			The P_b center at Si(111)-SiO_2 interface				
(ESR)							
Refs. 6, 7[e]	2.0011–2.0019	2.0080–2.0093	(1)	11	2.2		1.3
(Theory)							
Ref. 34[f]			1	15.2	2.1	3 NNN	1.0

[a]Measured by ENDOR.
[b]Calculated for the DB center in a relaxed a-Si_{110} cluster.
[c]Calculated for the FB center in relaxed a-Si_{81-86} clusters.
[d]Calculated for the DB center in relaxed a-$Si_{10-22}H_{15-27}$ clusters.
[e]Converted by A_{iso}, A_{aniso} (mT) $=0.1068\times A_{\text{iso}}$, A_{aniso} (10^{-4} cm^{-1}).
[f]Calculated for the DB center in an unrelaxed $Si_{22}H_{21}/Si_6O_{18}H_6$ cluster with spin polarization.

the main ^{29}Si hf interactions.[18] Thus, there will be two identifications for the DB center: (i) the doublet ^{29}Si hf structure should be observed in a $p=100$ at. % sample, and (ii) the intensity ratio of ^{29}Si hf lines and a primary line should amount to $p:1-p$. The observation of the doublet ^{29}Si hf structure in a 93 at. % ^{29}Si-enriched sample was consistent with the former identification.[8] In addition, our spectral simulations present the latter identification for the range of $p=1.6$–9.1 at. %. In contrast to the DB model, the FB model anticipated that there are two or three Si atoms where an unpaired electron is mainly located.[25] Therefore, the FB picture is inappropriate for explaining the present as well as previous results.

Different from the present study, Hikita *et al.* reported from spectral simulations on *X*-band ESR spectra that the primary line includes the ^{1}H hf structure with an isotropic hf splitting of 0.6 mT.[19] However, ESR measurements at quite low frequencies (<1 GHz) clarified that the hf splitting due to ^{1}H was estimated to be less than 0.1 mT.[8,29,30] In addition, we demonstrated that the whole DB spectrum and its dependence on ν and p can be calculated without a convolution of such a peculiar hf structure. Therefore, such a ^{1}H hf structure is unlikely to exist.

We found some differences in ESR parameters between the present and previous works on ESR. (i) Our $g_{\perp}$ was smaller than that of Stutzmann and Biegelsen by about 0.0015.[9] The 0.0015 difference in the g anisotropy yields a 0.9-mT difference in the width of spectrum at the Q band, so we could detect this difference. Accordingly, both $g_{\parallel}$ and $g_{\perp}$ were different from the case of the P_b center, which will be discussed in terms of the electronic structure of the defect later on. (ii) The estimated value of $A_{\text{iso-back}}$ was smaller than that obtained by electron-nuclear-double-resonance (ENDOR) measurement as well as an analysis on the signal broadening of ^{29}Si hf lines in a $p=93$ at. % sample.[8,11] Although estimations of $A_{\text{iso-back}}$ fluctuated among experiments because of the difficulty of estimating it accurately, the present and previous experiments agreed that $A_{\text{iso-back}}$ is much smaller than the main isotropic hf splitting A_{iso} of approximately 7.5 mT,[8,9,11] which also agrees with the theoretical simulation for the DB case.[18]

E. Microscopic structures of the DB

ESR parameters, especially hf parameters, are closely connected with the electronic and microscopic structures of the DB. For the cases of pure $3s$ and $3p$ orbitals of the Si atom, which are denoted by $|s\rangle$ and $|p\rangle$, respectively, A_{iso} and A_{aniso} have been theoretically calculated to be 149.0 and 3.6 mT, respectively.[31] Applying the LCAO expansion, the wave function $|\psi\rangle$ of an unpaired electron is written as

$$|\psi\rangle=\sum_i \alpha_i(\sigma_i|s\rangle+\pi_i|p\rangle), \tag{10}$$

where i indexes all atoms within the extent of $|\psi\rangle$ and the projection coefficients α_i, σ_i, and π_i obey the normalization conditions $\Sigma_i\alpha_i^2=1$, $\sigma_i^2+\pi_i^2=1$ for all i.[6–9] The localization strength at a threefold coordinated Si site $(i=1)\,\alpha_1^2$,

and $3s$ and $3p$ components on the site σ_1^2 and π_1^2, respectively, are approximately calculated as

$$\alpha_1^2 = 47-67\,\%, \tag{11a}$$

$$\sigma_1^2 = 6-9\,\%, \tag{11b}$$

and

$$\pi_1^2 = 91-94\%, \tag{11c}$$

by the same manner as previous studies.[6,7,9] Namely, the unpaired electron of the 2.0055 center is localized on a threefold-coordinated Si atom by more than one half of the total density and its character is almost p like.

For the case of the P_b center, it was concluded that $\alpha_1^2 = 80-84\%$, $\sigma_1^2 = 11-12\%$, and $\pi_1^2 = 88-89\%$.[6,7] A very similar s-p hybridization ratio in $g = 2.0055$ and the P_b centers indicates a similarity of the microscopic structure between the two centers. On the other hand, the two DB centers are different in regard to the localization strength, i.e., α_1^2; the 2.0055 center is much more delocalized than the P_b center.

When ϕ is defined to be the angle between the direction of $3p$ orbital of the DB and three backbonds, the value of ϕ is approximately given by $\cos\phi = -\sigma/\pi \times \sigma_1/\pi_1$, where σ^2/π^2 represents the s-p hybridization ratio of paired electrons of backbonds and now $\sigma^2/\pi^2 \sim \frac{1}{3}$. From this relation, ϕ is estimated to be about 100°, which is smaller than a normal tetrahedral angle of 109.27°. Thus, it is considered that the local structure of DB's is close to a planar structure such as a π electron on an sp^2 network plane rather than a normal tetrahedral structure in an sp^3 network. Likewise, the P_b center should have a similar structure to that of DB's in a-Si:H. Namely, it is considered that the threefold coordination in the Si network prefers such a planar configuration of Si atoms rather than the normal tetrahedral structure.

We recall the result that $W_{\rm iso}^A \sim 1.6$ mT and $W_{\rm aniso}^A \sim 1.1$ mT, which are different only by a factor of 2 from the case of ^{29}Si hf lines in the P_b spectrum where $W_{\rm iso}^A \sim 1.0$ mT and $W_{\rm aniso}^A \sim 0.7$ mT.[6,29] $W_{\rm iso}^A$ and $W_{\rm aniso}^A$, which represent the size of fluctuations of $A_{\rm iso}$ and $A_{\rm aniso}$, will indicate the degree of site-to-site variation of microscopic structure of DB's. Thus, in the vicinity of DB's, the degree of disorder seems to be similar between amorphous network and well-ordered Si(111)-SiO_2 interfaces.

The electronic structures of the DB are also considered in terms of the g shift. The g shift from a free-electron g value (2.0023) can be calculated by

$$\Delta g_{\mu\nu} = 2 \sum_{m \neq 0} \sum_i \frac{\langle \psi | L_\mu^{(i)} | m \rangle \langle m | \lambda_i(\mathbf{r}_i) L_\nu^{(i)} | \psi \rangle}{\varepsilon_0 - \varepsilon_m}, \tag{12}$$

where $|\psi\rangle$ is the DB wave function of the ground state, i.e., Eq. (10), and $|m\rangle$ represent that of excited states, ε_0 and ε_m are energies of the ground and excited states, respectively, λ_i is the spin-orbit coupling constant of an i atom, $\mathbf{r}_i$ is the position of the unpaired electron relative to an atom of i, and $L_{\mu,\nu}^{(i)}$ are components $(\mu, \nu = x,y,z)$ of orbital angular momentum operator with respect to a position of an i atom .[32] Immediately, it is clear that s orbitals do not contribute to the g shift because $L_\mu|s\rangle = 0$. Now, we consider the axis of symmetry to be the z axis. For the case of P_b center, $\Delta g_\parallel$ $(= \Delta g_{zz})$ was almost zero, while $\Delta g_\perp$ $(= \Delta g_{xx} = \Delta g_{yy})$ was as large as 0.007 (see Table II).[6,7] The fact that $\Delta g_\parallel = 0$ can be easily obtained from Eq. (12), because wave function $|\psi\rangle$ of the P_b center consists almost of a localized $3p_z$-orbital $|p_z\rangle$ and $L_z|p_z\rangle = 0$. On the other hand, $\Delta g_\perp$ will have a nonzero value because $L_{x,y}|p_z\rangle \neq 0$. A quantitative evaluation of Eq. (12) for a DB in Si clusters led to the result $\Delta g_\parallel \sim 0$ and $\Delta g_\perp > \Delta g_\parallel$.[33] For the 2.0055 center, we can find a similar relation in the g shift; $\Delta g_\parallel \sim 0.002$ and $\Delta g_\perp \sim 0.004$. Therefore, the DB picture was also suggested in terms of the g shift. The difference between $\Delta g_\parallel$ and $\Delta g_\perp$ reflects on the distribution widths of $g_\parallel$ and $g_\perp$, i.e., $W_\parallel^g$ and $W_\perp^g$, respectively. The fluctuation of $\Delta g_\parallel$ is not affected by the distribution of $\varepsilon_0 - \varepsilon_m|\psi\rangle$ and $|m\rangle$, in contrast to the case of $\Delta g_\perp$,[29] which brings about the relation $W_\parallel^g < W_\perp^g$. In fact, it was reported for the P_b signal that $W_\parallel^g$ was three times larger than $W_\perp^g$.[6,29] Likewise, in a-Si:H, $W_\parallel^g$ was estimated to be larger than $W_\perp^g$ [see Fig. 4(b)]. The reason why $\Delta g_\parallel$ deviates from zero in a-Si:H might be related with delocalization of the wave function of DB's. Since the DB wave function of a-Si:H is more spread out, we have to take into account the contributions of $L_z|p_{x,y}\rangle$ $(\neq 0)$ for atoms of $i \neq 1$, which will bring a nonzero contribution to $\Delta g_\parallel$. Furthermore, smaller $\Delta g_\perp$ in a-Si:H might be also ascribed to the smaller density of $|p_z\rangle$ at the DB site.

In estimating the unpaired electron populations on $3s$ and $3p$ orbitals of a Si atom in the singly occupied DB wave function, we did not consider the hf contribution from the spin densities, which might be induced by the effect of the spin polarization of bonding electrons and core electrons. The sign of hf interactions arising from the spin polarization is not necessarily the same as that of hf interactions due to the singly occupied DB wave function. For both cases of a-Si:H and the Si(111)/SiO_2 interface, the spin-dependent first-principles theoretical calculations predicted that the spin polarization increases the isotropic hf splitting,[34,35] so that the component of $3s$ orbital in the wave function σ_1^2 may be even smaller. Namely, the local structure of the DB may be a more planar structure, when the spin polarization is taken into account. In fact, a recent molecular dynamics simulation found completely planar DB's ($\phi \sim 90°$) in an amorphous $Si_{64}H_8$ supercell.[36]

IV. SUMMARY

Our objective was to confirm a previous conclusion on the dangling bond center ($g = 2.0055$) in undoped a-Si:H of Stutzmann and Biegelsen,[9] which was based on a simulation analysis of the spectrum obtained only by $\nu = 10$ GHz and $p = 4.7$ at. %, and was affected by a deconvolution procedure of ^{29}Si hf lines. For that purpose, we measured a variety of DB spectra using $\nu = 3-34$ GHz and samples with $p = 1.6$, 4.7, and 9.1 at. %, and also employed the echo-detected ESR technique of pulsed ESR as well as cw ESR. Using those ESR spectra, we carried out the spectral simulations on the whole dangling bond spectrum (a primary line and ^{29}Si hf lines) without the deconvolution of hf lines, and successfully reproduced the ν and p dependence of the DB spectra. The principal g values were obtained to be $g_\parallel = 2.0039$, $g_\perp$

$=2.0065$, and ^{29}Si hf splittings were determined to be $A_{iso}=6.9-7.9$ mT, $A_{aniso}=1.8-2.5$ mT, and $A_{iso\text{-}back}=1-2$ mT. The present ESR parameters were almost in good agreement with the results of Stutzmann and Biegelsen. Therefore, we confirmed their identification of $g=2.0055$ center for a wide range of two experimental parameters as well as free from the deconvolution problem. We pointed out that the dangling bond center of $g=2.0055$ has a quite similar bonding structure, electronic structure, and site-to-site variation to the dangling bond at $Si(111)/SiO_2$ interfaces (the P_b center) except for a much weaker localization of the $g=2.0055$ center.

ACKNOWLEDGMENTS

The authors are grateful to Dr. A. Matsuda for a variety of assistance and also Dr. S. Hayashi for his ^{1}H-NMR measurements. We thank Dr. N. Ishii and Dr. H. Katagiri for valuable discussions from a theoretical view point, and also Dr. J. K. Lee for his kindly help. This work, partly supported by NEDO, was performed in the Joint Research Center for Atom Technology (JRCAT) under the joint research agreement between the National Institute for Advanced Interdisciplinary Research (NAIR) and the Angstrom Technology Partnership (ATP).

[1] M. Brodsky and R. S. Title, Phys. Rev. Lett. **23**, 581 (1969).
[2] T. Shimizu, K. Nakazawa, M. Kumeda, and S. Ueda, Physica (Utrecht) **117B-118B**, 926 (1983).
[3] D. L. Staebler and C. R. Wronski, Appl. Phys. Lett. **31**, 292 (1977).
[4] H. Dersch, J. Stuke, and J. Beichler, Phys. Status Solidi B **105**, 265 (1981).
[5] S. Yamasaki, M. Kaneiwa, S. Kuroda, H. Okushi, and K. Tanaka, Phys. Rev. B **35**, 6471 (1987).
[6] K. L. Brower, Appl. Phys. Lett. **43**, 1111 (1983).
[7] W. E. Carlos, Appl. Phys. Lett. **50**, 1450 (1987).
[8] D. K. Biegelsen and M. Stutzmann, Phys. Rev. B **33**, 3006 (1986).
[9] M. Stutzmann and D. K. Biegelsen, Phys. Rev. B **40**, 9834 (1989); M. Stutzmann and D. K. Biegelsen, in *Amorphous Silicon and Related Materials*, edited by H. Fritzsche (World Scientific, Singapore, 1988), pp. 557–594.
[10] S. T. Pantelides, Phys. Rev. Lett. **57**, 2979 (1986).
[11] H. Yokomichi, I. Hirabayashi, and K. Morigaki, Solid State Commun. **61**, 697 (1987); H. Yokomichi and K. Morigaki, J. Non-Cryst. Solids **97-98**, 67 (1987).
[12] J. H. Stathis and S. T. Pantelides, Phys. Rev. B **37**, 6579 (1988).
[13] M. Stutzmann and D. K. Biegelsen, Phys. Rev. Lett. **60**, 1682 (1988).
[14] J. H. Sthathis, Phys. Rev. B **40**, 1232 (1989).
[15] P. A. Fedders and A. E. Carlsson, Phys. Rev. B **37**, 8506 (1988).
[16] N. Ishii and T. Shimizu, Jpn. J. Appl. Phys., Part 1 **27**, L1800 (1988).
[17] L. Martin-Moreno and J. A. Verges, Phys. Rev. B **39**, 3445 (1989).
[18] N. Ishii and T. Shimizu, Phys. Rev. B **42**, 9697 (1990).
[19] H. Hikita, K. Takeda, Y. Kimura, H. Yokomichi, and K. Morigaki, J. Non-Cryst. Solids **164-166**, 219 (1993); K. Morigaki, H. Hikita, M. Yamaguchi, and Y. Fujita, *ibid.* **227-230**, 338 (1998).
[20] J. Isoya, S. Yamasaki, H. Okushi, A. Matsuda, and K. Tanaka, Phys. Rev. B **47**, 7013 (1993).
[21] J. Isoya, S. Yamasaki, A. Matsuda, and K. Tanaka, Philos. Mag. B **69**, 263 (1994).
[22] S. Yamasaki and J. Isoya, J. Non-Cryst. Solids **164-166**, 169 (1993).
[23] L. D. Rollmann and S. I. Chan, in *Electron Spin Resonance of Metal Complexes*, edited by T. F. Yen (Plenum, New York, 1969), pp. 175–200.
[24] F. A. Cotton and E. Pedersen, Inorg. Chem. **14**, 382 (1975).
[25] K. L. Brower, Phys. Rev. B **33**, 4471 (1986).
[26] C. Kittel and E. Abrahams, Phys. Rev. **90**, 238 (1953).
[27] J. Humlícek, J. Quant. Spectrosc. Radiat. Transf. **27**, 437 (1982).
[28] J. J. Moré, in *Lecture Notes in Mathematics* Vol. 630, edited by G. A. Watson (Springer-Verlag, Berlin, 1977).
[29] S. Yamasaki, T. Umeda, J. H. Zhou, J. Isoya, and K. Tanaka, J. Non-Cryst. Solids **227-230**, 332 (1998).
[30] M. S. Brandt, M. W. Bayerl, M. Stutzmann, and C. F. O. Graeff, J. Non-Cryst. Solids **227-230**, 343 (1998).
[31] G. D. Watkins and J. W. Corbett, Phys. Rev. A **134**, 1359 (1964).
[32] A. J. Stone, Proc. R. Soc. London, Ser. A **271**, 424 (1963).
[33] H. Katagiri, Solid State Commun. **95**, 143 (1995).
[34] M. Cook and C. T. White, Phys. Rev. B **38**, 9674 (1988).
[35] N. Ishii and T. Shimizu, Solid State Commun. **102**, 647 (1997).
[36] N. Orita, T. Sasaki, and H. Katayama-Yoshida, in *Amorphous Silicon Technology-1993*, edited by E. A. Schiff, M. J. Thompsom, A. Madan, K. Tanaka, and P. G. LeComber, MRS Symposia Proceedings No. 297 (Materials Research Society, Pittsburgh, 1993), p. 171; Sci. Rep. Res. Inst. Tohoku Univ. A **39**, 33 (1993).